Field-Driven Translocation of Regular Block Copolymers through a Selective Liquid−Liquid Interface

A. Corsi,*,† A. Milchev,†,‡ V. G. Rostiashvili,† and T. A. Vilgis†

Max-Planck-Institute for Polymer Research, Ackermannweg 10, 55128 Mainz, Germany, and Institute for Physical Chemistry, Bulgarian Academy of Sciences, 1113 Sofia, Bulgaria

Received April 26, 2006; Revised Manuscript Received July 13, 2006

ABSTRACT: We propose a simple scaling theory describing the variation of the mean first passage time (MFPT) $\tau(N,M)$ of a regular block copolymer of chain length N and block size M which is dragged through a selective liquid−liquid interface by an external field B. The theory predicts a non-Arrhenian τ vs B relationship which depends strongly on the size of the blocks, M, and rather weakly on the total polymer length, N. The overall behavior is strongly influenced by the degree of selectivity between the two solvents χ. The variation of $\tau(N,M)$ with N and M in the regimes of weak and strong selectivity of the interface is also studied by means of computer simulations using a dynamic Monte Carlo coarse-grained model. Good qualitative agreement with theoretical predictions is found. The MFPT distribution is found to be well described by a Γ-distribution. Transition dynamics of ring and telechelic polymers is also examined and compared to that of the linear chains. The strong sensitivity of the "capture" time $\tau(N,M)$ with respect to block length M suggests a possible application as a new type of chromatography designed to separate and purify complex mixtures with different block sizes of the individual macromolecules.

1. Introduction

In a recent series of studies,[1−4] we have reported the results of comprehensive computer simulations which model the behavior of hydrophobic polar (HP) multiblock copolymers at a selective penetrable interface which divides two immiscible liquids, like water and oil, each of them being favored by one of the two types of monomers. As is well-known from experiment,[5−8] in the presence of selective interfaces for which the energy gain for a monomer in the favored solvent is large, the hydrophobic and polar blocks of a copolymer chain try to stay on different sides of the boundary between the two solvents, leading thus to a major reduction of the interfacial tension which has important technological applications, i.e., for compatilizers, thickeners, or emulsifiers. Not surprisingly, during the past two decades the problem has gained a lot of attention also from theory[9−13] as well as from computer experiment.[14−18] While in earlier studies attention has been mostly focused on diblock copolymers[6,8] due to their relatively simple structure, the scientific interest shifted later to random HP copolymers at penetrable interfaces.[10−13,18] In contrast, our investigations have focused mainly on the impact of block size M on the static properties and localization kinetics of regular multiblock copolymers at the phase boundary between the two immiscible solvents. We showed that these are well described by a simple scaling theory[1,3] in terms of the total copolymer length N (the number of repeating units in the chain), the block size M (the number of consecutive monomers of the same kind), and the selectivity parameter χ, that is, the energy gained by a monomer when moving into the more favorable solvent.

In the present work we extend our investigations to field-driven multiblock copolymers which cross the liquid−liquid interface and are temporarily trapped for a typical time $\tau(N,M)$. Our simulation results reveal a rich behavior of the drifting chains with qualitative differences in the two regimes of weak and strong selectivity χ. We demonstrate that a scaling theory may be designed which captures the main qualitative features of the mean first passage time $\tau(N,M)$ in terms of chain length N and block size M and provides insight into the complex behavior of the copolymer being dragged through the interface. We will show that the time $\tau(N,M)$ is very sensitive toward the block length M. This results can be viewed as a potential ground for the possible development of block-sensitive chramotography designed to separate complex copolymer mixtures. It is worthy of note that the dynamic Monte Carlo simulation, used in our study, does not take into account the hydrodynamic interactions. The role of hydrodynamic effects might be very important and deserves future investigation.

In section 2 we introduce our model and derive the main analytical results which describe the variation of translocation time with block size M and force strength B within the framework of Kramer's approximation for the first passage time. The main features of the Monte Carlo model which is used in our simulations are briefly sketched in section 3.1, while in section 3.2 we discuss the most salient results of our computer experiments. We end the paper with the main conclusions which the present investigation suggests.

2. Theory of Copolymer Detachment from the Interface

We now consider the model of translocation dynamics where a growing fraction of the chain is detached from the interface by the external field B and dragged into the underlying solvent, as shown schematically in Figure 1. The physical picture which provides the basis for our detachment model will be justified in section 3.2 by the direct visualization within the Monte Carlo simulation. This model will be used here to describe the characteristic time τ it takes to tear a string of blobs off the interface. To this end we calculate the free energy function.

2.1. Free Energy of the Detachment Model. We consider the free energy of the model, depicted in Figure 1, as a function of the instant length of the chain, m, which is in the lower half (**H**) of the container (the dangling end length). The total free

† Max-Planck-Institute for Polymer Research.
‡ Bulgarian Academy of Sciences.

10.1021/ma060920n CCC: $33.50
Published on Web 08/30/2006

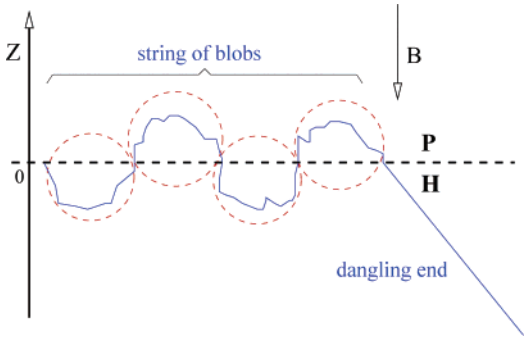

Figure 1. Schematic representation of the string of blobs subject to an external force *B*. In this scheme, the leading part of the chain (dangling end) is growing at the expense of the string of blobs still captured at the interface. **P** and **H** denote the polar and hydrophobic semispaces, respectively.

energy then contains the following terms:

$$\mathcal{F}(m) = \underbrace{F_{sel}(m) + F_{el}(m)}_{\text{dangling end free energy}} + F_{string}(m) \quad (1)$$

In this equation, $F_{sel}(m)$ and $F_{el}(m)$ are the selectivity interaction and the elastic deformation contributions of the leading end, whereas $F_{string}(m)$ is associated with the energy of the remaining string of blobs.

The selectivity energy of the dangling end is related to the interface potential and the HP copolymer binary sequence $\sigma(s)$ ($\sigma(s)$ assumes the values +1 and −1 depending on the nature of the monomer; see ref 1). In the hydrophobic semispace **H** ($z < 0$) this free energy reads

$$F_{sel}(m) = \frac{\chi}{2}\int_{N-m}^{N} ds\, \sigma(s) \quad (2)$$

A simple binary sequence for a multiblock copolymer with a block length of M can be constructed as $\sigma(s) = \sin[(\pi/M)s]$. Substituting this in eq 2 yields

$$F_{sel}(m) = -\frac{\chi M}{\pi}\sin^2\left(\frac{\pi m}{2M}\right) \quad (3)$$

where we have also taken into account that N and M have been chosen as multiples of 2 (as is usual in MC simulations).

2.1.1. Free Energy of Elastic Deformation. Here we consider the deformation energy of the different parts of the chain based on scaling arguments. We assume the interface position to be at $z = 0$. The external field acts uniformly on each polymeric segment with a force B which points in the negative z direction.

Each instantaneous configuration can be thought of as an array of loops which spread on both sides of the interface. We denote them as positive ($z > 0$) and negative ($z < 0$) loops. The two types of loops respond differently to the external field B. The positive loops are compressed, whereas the negative loops are stretched with respect to their equilibrium shape for $B = 0$ at the interface. Consider first the elastic free energy due to compression of a positive loop. Suppose a loop of a length n runs in the positive direction up to a height h. Then the elastic free energy can be written as

$$F^{(+)}(n,h) \simeq Tn\left(\frac{a}{h}\right)^{1/\nu} + \frac{2B}{a}\int_0^h z\, dz \simeq Tn\left(\frac{a}{h}\right)^{1/\nu} + \frac{Bh^2}{a} \quad (4)$$

The first term on the right-hand side of eq 4 is due to confinement entropy, whereas the second one is related to the external field energy; T stands for the temperature, and a denotes the Kuhn segments length. Optimizing eq 4 with respect to h, one gets $h_0/a = (nT/aB)^{\nu/(1+2\nu)}$, which substituted back into eq 4 gives

$$F^{(+)}(n) \simeq T\left(\frac{aB}{T}\right)^{1/(1+2\nu)} n^{2\nu/(1+2\nu)} \quad (5)$$

Let us now look at the stretching free energy associated with the deformation of the a negative loops. The elongation of a chain in a good solvent due to forces f applied at both ends,[19] for small extensions, $an^\nu < h \ll an$, reads

$$h \simeq \begin{cases} a^2 n^{2\nu} f/T & f \ll T/an^\nu \\ an(af/T)^{(1/\nu)-1} & f \gg T/an^\nu \end{cases} \quad (6)$$

Following Brochard-Wyart et al.[20−22] (see also the Monte Carlo simulation in the wake of these results),[23] one may describe the nonuniform stretching of tethered chains in the differential form $dh(s)/ds \simeq a(fa/T)^{(1/\nu)-1}$, where s is the running curvilinear coordinate of a polymeric segment and the field B acts on each monomer. The total force is then $f = sB$. The elongation of a string with n monomers is then obtained from $dh(s)/ds \simeq a(Bsa/T)^{(1/\nu)-1}$ by integration of s, $0 \le s \le n$, and yields

$$h \simeq an^{1/\nu}\left(\frac{aB}{T}\right)^{(1/\nu)-1} \quad (7)$$

This result is valid for fairly large forces $nB > T/an^\nu$ or $B > T/an^{\nu+1}$, which exceed the thermal agitation. On the other hand, the Pincus blob size cannot be smaller than the Kuhn length, i.e., $nB < T/a$ or $B < T/an$. As a result, the deformation law[7] is valid for forces in the interval $T/n^{\nu+1} < B < T/an$. The corresponding free energy of stretching takes the form

$$F^{(-)}(n) \simeq \int_0^n f\frac{dh}{ds}\, ds \simeq a\left(\frac{aB}{T}\right)^{(1/\nu)-1} B\int_0^n s^{1/\nu}\, ds \simeq T\left(\frac{aB}{T}\right)^{1/\nu} n^{(1/\nu)+1} \quad (8)$$

In the weak field regime, $B < T/an^{\nu+1}$, the elongation law follows from the first line of eq 4, i.e., $dh(s)/ds \simeq a(aB/T)s^{2\nu}$, and the resulting stretching free energy becomes

$$F^{(-)}(n) \simeq \int_0^n f\frac{dh}{ds}\, ds \simeq a\left(\frac{aB}{T}\right)B\int_0^n s^{2\nu+1}\, ds \simeq T\left(\frac{aB}{T}\right)^2 n^{2\nu+2} \quad (9)$$

Thus, the elastic free energy in both weak and relatively strong stretching regimes (see eqs 9 and 8) is given by

$$F^{(-)}(n) \simeq \begin{cases} T\left(\frac{aB}{T}\right)^2 n^{2\nu+2}, & \text{if } B < \frac{T}{an^{\nu+1}} \\ T\left(\frac{aB}{T}\right)^{1/\nu} n^{(1/\nu)+1}, & \text{if } \frac{T}{an^{\nu+1}} < B < \frac{T}{an} \end{cases} \quad (10)$$

2.1.2. Total Free Energy. From the previous section we have for the elastic free energy of the leading part which includes m monomers of the dragged chain, according to eq 10

$$F_{el}(m) \simeq -T\left(\frac{aB}{T}\right)^{1/\nu} m^{(1/\nu)+1} \quad (11)$$

The negative sign here implies that the chain moves downhill along the external field.

Consider now the free energy of the string of blobs, that is, of the rest of the copolymer which is still trapped at the interface. The length of such a blob at the interface is[1]

$$g \simeq \chi^{-2/(1-\nu)} M^{-(1+\nu)/(1-\nu)} \tag{12}$$

whereby the blobs are placed alternatively in the *P* or *H* sides of the interface. Each blob has an energy of the order of *T*. The number of blobs is $(N - m)/g$ with g the number of (both *H* and *P*) monomers in a blob. Taking into account the expressions for the elastic energy (5) and (10), the free energy of the string of blobs is proportional to

$$F_{\text{string}}(m) \simeq -T\left(\frac{N-m}{g}\right) + \alpha_1 T\left(\frac{N-m}{2g}\right)\left(\frac{aB}{T}\right)^{\gamma} g^{1-\gamma} + \alpha_2 T\left(\frac{N-m}{2g}\right)\left(\frac{aB}{T}\right)^{1/\nu} g^{(1/\nu)+1}$$

$$\simeq -T(N-m)\left[\frac{1}{g} - \frac{\alpha_1}{2}\left(\frac{aB}{Tg}\right)^{\gamma} - \frac{\alpha_2}{2}\left(\frac{aBg}{T}\right)^{1/\nu}\right] \tag{13}$$

where α_1 and α_2 are some numeric factors and $\gamma = 1/(1 + 2\nu)$. The first term in eq 13 is associated with the energy of localization (therefore it is negative), whereas the two other terms are due to the elastic deformation of blobs.

In the strong localization limit the positive and negative loops which constitute the string of blobs are of length *M*. The localization energy for each loop is $F_{\text{loc}} \simeq -\chi M$, whereas the number of loops is $(N - m)/M$. Thus, the free energy of the string of the loops reads

$$F_{\text{string}}(m) \simeq -\chi(N-m) + \beta_1 T\left(\frac{N-m}{2M}\right)\left(\frac{aB}{T}\right)^{\gamma} M^{1-\gamma} + \gamma_2 T\left(\frac{N-m}{2M}\right)\left(\frac{aB}{T}\right)^{1/\nu} M^{(1/\nu)+1}$$

$$\simeq -T(N-m)\left[\frac{\chi}{T} - \frac{\beta_1}{2}\left(\frac{aB}{TM}\right)^{\gamma} - \frac{\beta_2}{2}\left(\frac{aBM}{T}\right)^{1/\nu}\right] \tag{14}$$

where β_1 and β_2 are constant factors.

With eqs 3, 11, 13 and 14, the total free energy (eq 1) reads

$$\mathcal{F}(m) \simeq -\frac{\chi M}{\pi}\sin^2\left(\frac{\pi m}{2M}\right) - T\left(\frac{aB}{T}\right)^{1/\nu} m^{(1/\nu)+1} - T(N-m)\begin{cases}\left[\frac{1}{g} - \frac{\alpha_1}{2}\left(\frac{aB}{Tg}\right)^{\gamma} - \frac{\alpha_2}{2}\left(\frac{aBg}{T}\right)^{1/\nu}\right] & \text{for weak localization}\\ \left[\frac{\chi}{T} - \frac{\beta_1}{2}\left(\frac{aB}{TM}\right)^{\gamma} - \frac{\beta_2}{2}\left(\frac{aBM}{T}\right)^{1/\nu}\right] & \text{for strong localization}\end{cases} \tag{15}$$

The expression in square brackets of eq 15 (for the case of the weak localization limit) can be viewed as an inverse effective blob size $1/g$, i.e.

$$\frac{1}{q} \equiv \frac{1}{g} - \frac{\alpha_1}{2}\left(\frac{aB}{Tg}\right)^{\gamma} - \frac{\alpha_2}{2}\left(\frac{aBg}{T}\right)^{1/\nu} \tag{16}$$

The significant difference between the weak and strong localizations which is pointed out in eq 15 will become apparent in section 2.2.4. Namely, there we will show that the characteristic translocation time for the weak localization regime grows monotone with the block length *M*, whereas in the strong localization case this dependence passes through the maximum.

2.2. Translocation Time. 2.2.1. Preliminaries. It is well-known that the one-dimensional Smoluchovsky problem allows for an exact analytical solution for the mean first passage time.[24−26] Let us assume that a stochastic process $\xi(t)$ which describes the drift diffusion of a chain in the external field $U(x)$ extends between the boundaries x_1 or x_2, provided that $\xi(0) = x_0$.

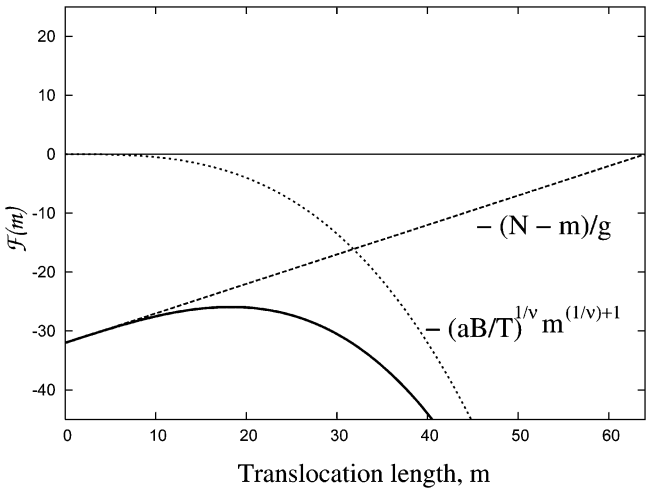

Figure 2. Schematic representation of the total free energy (solid line). The dashed line and the dotted line represent the localization energy and the elastic energy, respectively.

Then the expression for the mean passage time $\tau(x_0)$ has the form

$$\tau(x_0) = \int_{x_0}^{x_2} dx' \frac{e^{\beta U(x')}}{D(x')} \int_{x_1}^{x'} dy\, e^{-\beta U(y)} \tag{17}$$

where $D(x)$ is the corresponding diffusion coefficient. In view of the results of the previous section, we can map the problem at hand onto the one-dimensional Smoluchovsky problem where the corresponding free energy $\mathcal{F}(m)$ plays the role of an external potential. The question about the choice of the proper diffusion coefficient *D* is more open. Considering the translocation through a nanopore, Park and Sung[27−29] suggested that *D* should be identified with the Rouse model diffusion coefficient which scales as $D = D_0/N$. On the other hand, Muthukumar[30] assumed that *D* is not the diffusion coefficient of the whole chain but rather the diffusion coefficient of the monomer which just passes the pore, and hence a constant, independent of *N* (see also an interesting discussion in ref 31). We will consider here *D* as a free parameter and will use a correspondence principle (see below) in order to fix it. We are interested in the average first-passage time when the length *m* changes within the interval $1 \le m \le N - 1$. Using eq 17, this time can be written in the form

$$\tau(1 \to N-1) = \frac{a^2}{D(N)} \int_1^{N-1} dm\, e^{\beta \mathcal{F}(m)} \int_1^{m} dn\, e^{-\beta \mathcal{F}(n)} \tag{18}$$

We emphasize that this expression is basically valid under conditions when the chain is initially in equilibrium at the interface. The completely opposite case is that of a chain that is dragged through the interface while being in the steady-state conformation typical of a drifting coil. The treatment of the latter case is more complicated and might not be simply based on the use of the same free energy, unless the dragging motion is pretty slow.

2.2.2. Kramer's Escape Time. One may simplify the double integral of eq 18 to treat it analytically. To this end only two important terms in eq 15 can be left: the localization energy, $-(N - m)/q$, and the elastic energy, $-(aB/T)^{1/\nu} m^{(1/\nu)+1}$, the latter being responsible for the detachment. Then the resulting free energy function is shown in Figure 2.

As one can see, the resulting barrier closely resembles that of the Kramer's escape problem.[24] In order to roughly estimate

the escape time and its dependence on B, N, and M, we assume that the barrier determines the escape time. This means that the slowest part of the process is related to the barrier surmounting, whereas the rest of the translocation goes much faster. The free energy functional in this case has the form

$$\mathscr{F}(m) \simeq -T\frac{N-m}{q} - T\left(\frac{aB}{T}\right)^{1/\nu} m^{(1/\nu)+1} \tag{19}$$

which has a maximum at $m^* \simeq (\gamma_1/q^\nu)(T/aB)$ where the numeric coefficient $\gamma_1 = 1/(1+1/\upsilon)^\nu$. The condition that m^* cannot be larger than N leads to the restriction $aB/T \geq \gamma_1/q^\nu N$. The corresponding free energy maximum value is given by

$$\mathscr{F}(m^*) = -\frac{N}{q} + \frac{\gamma_2}{q^{1+\nu}}\left(\frac{T}{aB}\right) \simeq -\frac{N-m^*}{q} \tag{20}$$

where $\gamma_2 = 1/(\upsilon(1+1/\upsilon)^{1+\nu})$.

The integral over m in eq 18 gets its main contribution at $m \simeq m^*$, so that we replace the factor $\exp\{\beta\mathscr{F}(m)\}$ by $\exp\{\beta\mathscr{F}(m^*) - \beta|\mathscr{F}''(m^*)|(m-m^*)^2/2\}$, where $\beta\mathscr{F}''(m^*) \simeq -(aB/T)^{1/\nu}(m^*)^{(1/\nu)-1}$. Now, as $m \simeq m^*$, the main contribution in the integral over n comes from the area $n \simeq 0$ (we have assumed for simplicity that the low integration limit equals zero). Then, $\exp\{\beta\mathscr{F}(n)\} = \exp\{-\beta\mathscr{F}(0) - \beta\mathscr{F}'(0)n\}$, where $\beta\mathscr{F}(0) \simeq -N/q$ and $\beta\mathscr{F}'(0) \simeq 1/q$. After taking all these expansions into account, the integrals in eq 18 can be easily calculated, and the result has the following form:

$$\tau \simeq q^{(3-\nu)/2}\left(\frac{a^2}{D}\right)\left(\frac{T}{aB}\right)^{1/2} \exp\left[\frac{1}{q^{1+\nu}}\left(\frac{T}{aB}\right)\right] \tag{21}$$

The following comments are noteworthy in connection with this result. The exponential term has the form of an Arrhenius factor $\exp(m^*/q)$, where m^*/q is the barrier height (see the solid line in Figure 2). The resulting B dependence of $\ln\tau$ appears as $\ln\tau \sim T/(aB)$, which qualitatively agrees with the MC simulations findings (see below). At $B \to 0$ one has $m^* \to N$ (it can be seen in Figure 2), and the activation energy is simply equal to the localization free energy of the full chain $F_{\mathrm{loc}} \sim N/g$ (see the corresponding result in ref 1), as it should be.

2.2.3. Unperturbed Drift. As noted above, we will treat the coefficient D in eq 21 as a free parameter which can be fixed by taking advantage of the correspondence principle. In our case this principle states that for a sufficiently large external force B the activation barrier disappears, and one observes a pure drift of the chain. As one can see from eq 15, this happens when $1/q \ll 1$. Then the interface crossing τ_{drag} is mainly defined by the balance of the Stokes friction and external forces, i.e., $\zeta_0 N v_{\mathrm{c.m.}} = NB$, where ζ_0 is the Stokes friction coefficient and $v_{\mathrm{c.m.}}$ is the velocity of the chain's center of mass, given by the formula $v_{\mathrm{c.m.}} = B/\zeta_0$. The effective thickness of the interface in this case is of the order of the blob length, i.e., $\xi \simeq ag^\nu$, and the time τ_{drag} can be estimated as $\tau_{\mathrm{drag}} \simeq ag^\nu/B\,\zeta_0$. Then we can adopt τ_{drag} as a preexponent factor in the Kramer's escape time relation, i.e.

$$\tau \simeq g^\nu\left(\frac{\zeta_0 a^2}{T}\right)\left(\frac{T}{aB}\right) \exp\left\{\frac{1}{q^{1+\nu}}\left(\frac{T}{aB}\right)\right\} \tag{22}$$

In the more general case we should deal with the complete full double integral of eq 18. Once again, in this limit the second term in eq 19 prevails, and we have

$$\tau = \frac{a^2}{D}\int_0^N \mathrm{d}m\, \exp\left\{-\left(\frac{aB}{T}\right)^{1/\nu} m^{(1/\nu)+1}\right\} \times \int_0^m \mathrm{d}n\, \exp\left\{\left(\frac{aB}{T}\right)^{1/\nu} n^{(1/\nu)+1}\right\} \tag{23}$$

It is convenient to substitute the variables in both integrals with $x = (aB/T)^{1/\nu}m^{(1/\nu)+1}$ and $y = (aB/T)^{1/\nu}n^{(1/\nu)+1}$. The resulting expression reads

$$\tau = \frac{a^2}{D}\left(\frac{T}{aB}\right)\int_0^\infty \mathrm{d}y\, \frac{\mathrm{e}^{-\gamma}}{y^{1/(1+\nu)}}\int_0^y \mathrm{d}x\, \frac{\mathrm{e}^x}{x^{1/(1+\nu)}} \tag{24}$$

By setting the upper limit in the integral over y equal to infinity, we keep in mind that this integral converges as $y \to \infty$ so that it does not depend on N at large N. This convergence can be easily seen if we take into account the behavior of the integral over x for small and large y values, i.e.

$$\int_0^y \mathrm{d}x\, \frac{\mathrm{e}^x}{x^{1/(1+\nu)}} \simeq \begin{cases} \mathrm{e}^y/y^{1/(1+\nu)} & \text{for } y \gg 1 \\ y^{\nu/(1+\nu)} & \text{for } y \ll 1 \end{cases} \tag{25}$$

The correspondence to the pure drift regime leads us to the conclusion that the factor in front of the integral in eq 24 should be equal to τ_{drag} (from $\tau_{\mathrm{drag}} = ag^\nu\zeta_0/B$). This enables us to fix the coefficient D as

$$D = \frac{1}{g^\nu}\left(\frac{T}{\zeta_0}\right)\left(\frac{T}{aB}\right)^{(1-\nu)/(1+\nu)} \tag{26}$$

Finally, we need to point out that the equation for dragging time can be derived differently starting from the first passage time formula[17] (see Appendix).

2.2.4. Numerical Analysis. For a first assessment of our theoretical treatment we present below some numerical calculations based on the Kramer's escape time expression.[22] First and foremost, we calculate the expression for the blob length $g(\chi,M)$ which is of great importance in eq 15 for the total free energy. The number of monomers g in the blob can be written as $g(\chi,M) = N[(\chi_c(M,N)/\chi]^{2/(1-\nu)}$, where the crossover selectivity χ_c has been extensively discussed in ref 1, and its scaling is $\chi_c \sim M^{-(1+\nu)/2}N^{-(1-\nu)/2}$. The substitution of this χ_c in g leads back to eq 12. The characteristic point where the blob length becomes of the order of the block length M is the strong localization threshold χ_∞. Here we will use for χ_c and χ_∞ the typical values obtained from Monte Carlo simulations.[1] The corresponding data are given in Table 1. The subsequent calculations of the Kramer's escape time in the weak localization regime are done for a selectivity parameter $\chi = 1.2$.

We have used these data in the case $N = 128$ to make a 3D plot of g, which is shown in Figure 3. The contour lines in the $\chi-M$ plane of Figure 3 illustrate the narrow region of M-dependent selectivity strength where a crossover from weak to strong localization of the copolymer at the interface occurs. At the critical selectivity $\chi_c(M)$ the blobs reach the largest size $g \approx N$, which involves nearly all monomers N, whereas with further increase of χ the blob size rapidly decreases, and at the onset of the strong localization, χ_∞, it reduces to the size of an individual block M. As demonstrated below, within the narrow interval of weak localization, $\chi_c(M) \leq \chi \leq \chi_\infty(M)$, confined between the outermost contour lines in Figure 3 as well as in the vast region of strong localization, $\chi \geq \chi_\infty$, both our theory and the simulations show a qualitatively different behavior of the translocation time with respect to B and M in the two regions.

The implementation of $g(\chi,M)$ in the equation for Kramer's escape time[22] (where $1/q$ is given by eq 16) leads to a τ vs B

Table 1. Weak and Strong Localization Thresholds Data

	weak localization threshold χ_c					strong localization threshold χ_∞					
	$N = 32$	$N = 64$	$N = 128$	$N = 256$	$N = 512$		$N = 32$	$N = 64$	$N = 128$	$N = 256$	$N = 512$
$M = 1$	1.8003	1.5572	1.3467	1.1670	1.0083	$M = 1$	3.7495	3.4189	2.9835	2.9022	3.2040
$M = 2$	1.5689	1.2902	1.0511	0.9591	0.9281	$M = 2$	2.9507	2.8744	2.3954	2.1838	2.5536
$M = 4$	1.0157	0.9309	0.7379	0.6601	0.6526	$M = 4$	2.0357	1.8855	1.6941	1.5616	1.6459
$M = 8$	0.7573	0.5851	0.4675	0.3405	0.2767	$M = 8$	1.1484	1.1115	1.0688	1.0337	0.9187
$M = 16$		0.2984	0.2900	0.1708	0.1720	$M = 16$		0.5593	0.5645	0.5358	0.5403
$M = 32$			0.2091	0.0829	0.0604	$M = 32$			0.3603	0.2608	0.2941
$M = 64$					0.0524	$M = 64$					0.1288

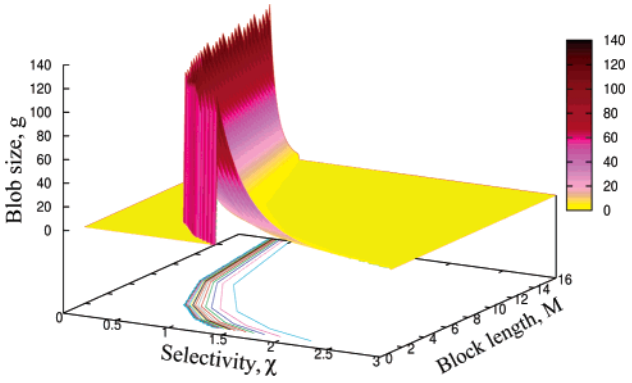

Figure 3. Variation of the blob size g with block length M for various degrees of interface selectivity χ. The contour lines demark the region of selectivity values in which a gradual transition from weak to strong localization takes place. At $\chi_c(M)$ (the first contour line on the left) one has $g \approx N$ (here $N = 128$), while at χ_∞ (last contour line on the right) the blob coincides with the block size M.

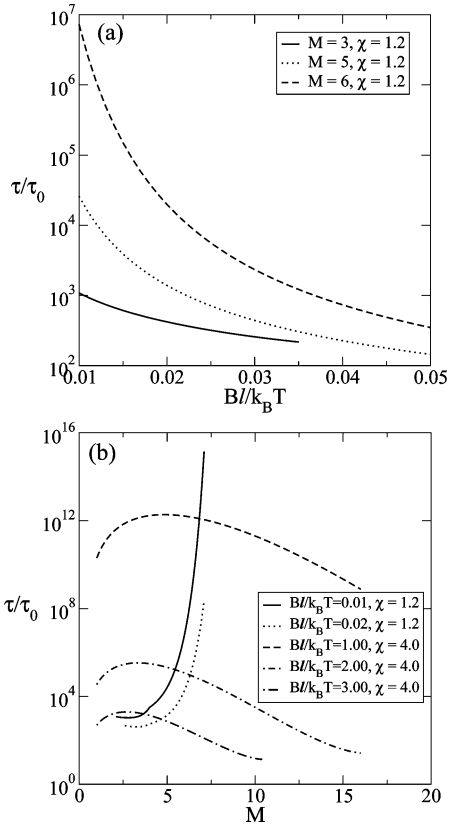

Figure 4. (a) τ/τ_0 vs dragging force B for several block sizes M. (b) τ/τ_0 vs M in the regime of weak localization, $\chi = 1.2$, and strong localization, $\chi = 4.0$, and several values of the external field B.

relationship, which is given in Figure 4a. One can readily verify that this relationship is of non-Arrhenian type, which implies that the height of the activation barrier for crossing the interface varies with the variation of the dragging force B. Evidently, with growing block size M this non-Arrhenian behavior becomes progressively more pronounced. We will see later that this is consistent with MC results and that the non-Arrhenian variation of τ with B becomes also progressively enhanced as the chain length N grows.

Figure 4b displays the variation of τ with M for several values of the force B in the regimes of weak and strong localization. One can see that the τ vs M relationship differs qualitatively between the two cases. In the weak localization regime one finds a very steep (by orders of magnitude) monotonous increase of τ with M, i.e., the escape time is strongly selective with respect to the block size. In contrast, in the strong selectivity regime, $\chi = 4.0$, the change of τ with M is non-monotonous (it goes through a maximum) and is not so strong. This is a result of the different responses of positive and negative loops to the external field B as discussed in section 2.1.2.

3. Monte Carlo Simulations

3.1. Simulation Model. The off-lattice bead−spring model employed during our study has been previously used for simulations of polymers both in the bulk[32,33] and near confining surfaces;[34−39] thus, we describe here the salient features only. Each polymer chain contains N effective monomers connected by anharmonic springs described by the finitely extendible nonlinear elastic (FENE) potential.

$$U_{\mathrm{FENE}} = -\frac{K}{2}R^2 \ln\left[1 - \frac{(l - l_0)^2}{R^2}\right] \tag{27}$$

Here l is the length of an effective bond, which can vary in between $l_{\min} < l < l_{\max}$, with $l_{\min} = 0.4$, $l_{\max} = 1$ being the unit of length, and has the equilibrium value $l_0 = 0.7$, while $R = l_{\max} - l_0 = l_0 - l_{\min} = 0.3$, and the spring constant K is taken as $K/k_BT = 40$. The nonbonded interactions between the effective monomers are described by the Morse potential

$$U_{\mathrm{M}} = \epsilon_{\mathrm{M}}\{\exp[-2\alpha(r - r_{\min})] - 2\exp[-\alpha(r - r_{\min})]\} \tag{28}$$

where r is the distance between the beads, and the parameters are chosen as $r_{\min} = 0.8$, $\epsilon_{\mathrm{M}} = 1$, and $\alpha = 24$. Owing to the large value of the latter constant, $U_{\mathrm{M}}(r)$ decays to zero very rapidly for $r > r_{\min}$ and is completely negligible for distances larger than unity. This choice of parameters is useful from a computational point of view, since it allows the use of a very efficient link-cell algorithm.[40] From a physical point of view, these potentials eqs 27 and 28 make sense when one interprets the effective bonds as Kuhn segments, comprising a number of chemical monomers along the chain, and thus the length unit $l_{\max} = 1$ corresponds physically rather to 1 nm than to the length of a covalent C−C bond (which would only be about 1.5 Å). Since in the present study we are concerned with the localization of a copolymer in good solvent conditions, in eq 28 we retain the repulsive branch of the Morse potential only by setting $U_{\mathrm{M}}(r) = 0$ $r > r_{\min}$ and shifting $U_{\mathrm{M}}(r)$ up by ϵ_{M}.

CDV

The interface potential is taken simply as a step function with amplitude χ

$$U_{\text{int}}(n,z) = \begin{cases} -\sigma(n)\chi/2 & z > 0 \\ \sigma(n)\chi/2 & z \le 0 \end{cases} \tag{29}$$

where the interface plane is fixed at $z = 0$, and as explained before, $\sigma(n) = \pm 1$ denotes a "spin" variable which distinguishes between P and H monomers. The energy gain of each chain segment is thus $-\chi$, provided it stays in its preferred solvent.

During each Monte Carlo update, a monomer is chosen at random, and one attempts to displace it randomly by displacements Δx, Δy, Δz chosen uniformly from the intervals $-0.5 \le \Delta x, \Delta y, z \le 0.5$. The transition probability for such an attempted move is simply calculated from the total change ΔE of the potential energies defined in eqs 27−29 as $W = \exp(-\Delta E/k_BT)$. According to the standard Metropolis algorithm, the attempted move is accepted only if W exceeds a random number uniformly distributed between zero and unity. Since our potentials are constructed such that chains cannot intersect themselves in the course of random displacement of beads, one does not need to check separately for entanglement restrictions.

One should point out that the external field B, which imposes a bias in the random hops performed by the chain monomers, should be taken in the simulation sufficiently weak,[41] $B\Delta Z \ll k_BT$. Indeed, the field B whose only component is directed along the negative Z-axis enters as an additional term in the Boltzmann factor, $\delta E = B\Delta Z$, which makes the energy a steadily decreasing function of Z. The Metropolis algorithm thus drives the polymer chain toward an unreached (and unreachable) minimum which produces a uniform drift downward. The average jump distance in a dilute system $\langle \Delta Z \rangle \approx 1/4$, no matter how strong the applied field is chosen.[41] Thus, for large B the probability of a jump along the field quickly saturates at unity so that any further increase of B would not really lead to higher drift velocity of the polymer.

In the course of the simulation the starting configuration of the copolymer is relaxed for a period of time and then placed at the ceiling of our simulation box before the field B acting in vertical direction is switched on. The onset of the translocation process is defined as the time when the first monomer of the drifting chain touches the interface and the moment when the last monomer leaves the upper half of the box and then denotes the end of the process. Since the time τ during which the chain remains in contact with the interface fluctuates considerably, for all chains of length $16 \le N \le 256$ we take averages over 1000 simulation runs.

3.2. Discussion of Monte Carlo Results. In section 2 we assumed a mechanism of copolymer detachment from the interface which have lead us to predict a non-Arrhenian variation of the time τ with the imposed field B. We demonstrated that a selective liquid−liquid interface can be very sensitive with respect to the block size M of a multiblock copolymer chain. On the other hand, as shown in the Appendix, the N dependence of τ is rather weak and nearly vanishes in the limit of long chains. In order to test the predictions of the analytic theory and deepen our understanding of the overall picture of translocation through a liquid interface, we report in the present section the results of some extensive Monte Carlo simulation by means of the model described in section 3.

In Figure 5 we show the distribution of capture times $P(\tau)$, measured for a copolymer in the weak localization regime, for three different field strengths. Despite the considerable scatter in data which remains after 1000 measurements, evidently these distributions are shown to collapse on a single "master" curve when scaled by the mean capture time $\langle \tau(B) \rangle$. The solid line in Figure 5 corresponds to a Γ-distribution. This distribution arises naturally in processes for which the waiting times between Poisson distributed events are relevant.

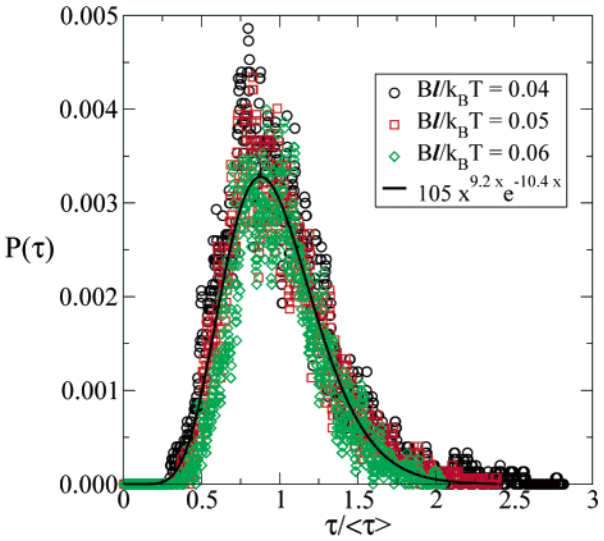

Figure 5. Master plot of the distribution of capture times $P(\tau)$ vs $\tau/\langle\tau\rangle$ for a copolymer chain with $N = 128$, $M = 4$ at $\chi = 1.5$ for three different fields B, as indicated. The time intervals have been scaled by the value of $\langle\tau\rangle$ appropriate for the respective value of the field B. A full line denotes the best fit of a Γ-distribution.

One of the main results of our computer experiments is displayed in Figure 6, where the variation of $\langle\tau\rangle$ with the bias B is plotted for chains of different length N and fixed block size $M = 4$ in semilog coordinates. A general feature, evident from Figure 6a, is the well expressed non-Arrhenian $\langle\tau\rangle$ vs Bl/k_BT relationship which confirms our expectations from section 2 (see Figure 4). From Figure 6a it becomes evident that this non-Arrhenian-type relationship crosses over to Arrhenian one for shorter chain ($N = 16, 32$) where insufficient length prevents the formation of (large) blobs of size g as expected at criticality $\chi_c = 1.5$. For sufficiently long copolymers, $N \ge 64$, in contrast, the capture time τ depends only weakly on chain length N, and the τ vs B relationship remains qualitatively unchanged. This suggests that the activation barrier, which has to be overcome when a chain is detached from the interface by the field, grows with decreasing drift velocity. One could imagine that in a strong field B the copolymer moves so fast that the translocation time is much shorter than the time it takes for the polymer to localize at the phase boundary and attain its lowest free energy. For small values of Bl/k_BT, in contrast, the copolymer has sufficient time to attain full equilibrium at the selective interface, and the corresponding potential well in which the chain resides gets deeper. While the non-Arrhenian τ vs Bl/k_BT relationship is also observed in the case of strongly selective phase boundary, Figure 6b, qualitatively the variation of τ with chain length N looks quite different. While at both ends of the interval of variation of B the capture time practically does not depend on N, in the intermediate region, $0.4 \le Bl/k_BT \le 0.8$, the longer chains spend less time at the interface than the shorter ones! At present we lack a reliable explanation for this effect. One might assume, however, that in this interval of intermediate B intensities the process of copolymer detachment is governed by the probability for the formation of a critical protuberance. Such a probability should then be proportional to the total chain length N. Considerations of this kind indicate, however, the necessity of a more detailed information about the underlying mechanism of copolymer detachment and its temporal evolution. Therefore,

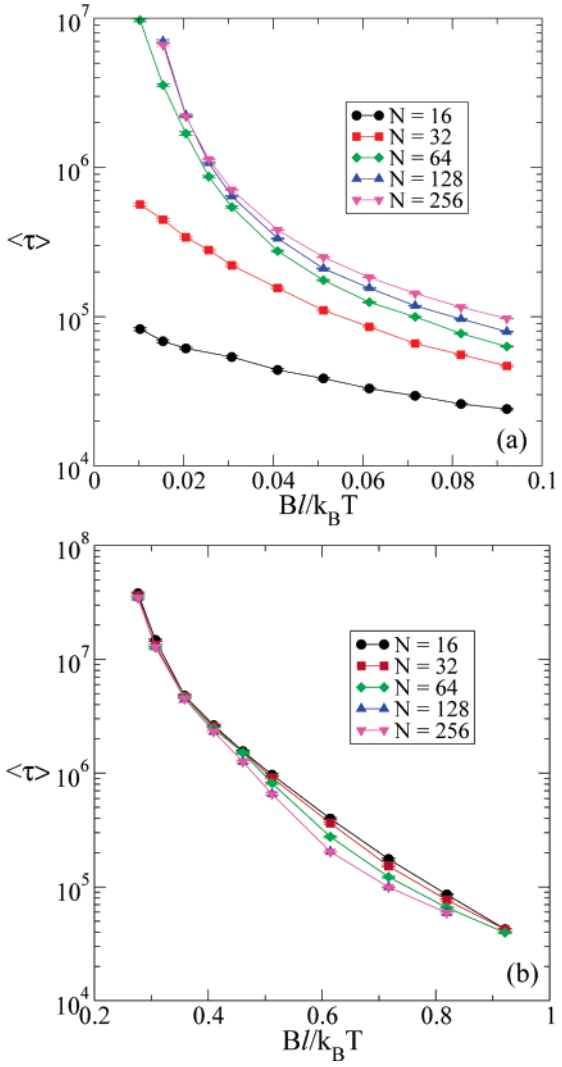

Figure 6. (a) Variation of τ vs dragging force B for chain lengths $N = 16$, 32, 64, 128, and 256 in the weak localization regime $\chi = 1.5$. (b) The same as in (a) in the regime of strong localization, $\chi = 4.0$.

in Figure 7 we present a series of snapshots which capture the time history of detachment by depicting the instantaneous positions of all repeat units of the chain at four successive times after the onset of one particular translocation. One can clearly see in Figure 7 that after an initial latent period a protuberance is formed at the free (dangling) end of the chain between monomers $120 \leq n \leq 128$ which from the start is immersed in its preferred solvent. After 20 000 MCS this end evolves into a progressively growing protuberance which eventually tears off the copolymer from the interface and drags it into the lower half of the simulation box. Our observation shows, however, that such protuberances form occasionally everywhere along the backbone of the chain and then die out with time or grow spontaneously like an avalanche. Thus, the analogy with the mechanism of detachment, envisaged in our theoretical treatment, section 2, should be apparent. We note here that in order to check the role which the dangling end of the chain plays in assisting the detachment process we also made test runs with ring copolymers (see below) under otherwise equivalent conditions and found no qualitatively different behavior when dangling ends are eliminated.

An important test for the theory, as developed in section 2, is represented by the analysis of the block size dependence of the translocation time $\tau(M)$. In Figure 8a we demonstrate the extremely strong sensitivity of τ on M for the case of weak selectivity, $\chi = 1.5$, which leads to a steady increase in τ by more than a decade with doubling the block size. Figure 8a also suggests that this sensitivity gets fully pronounced for sufficiently long chains, $N \geq 64$, which we attribute to the formation of sufficiently large blobs unrestricted by the finite size of the copolymer. The variation of the translocation time with block size M for a fixed field strength $B = 0.3$, 0.5, and 0.7 is shown in 8b where the steep (nearly exponential) increase is evident. Qualitatively the observed behavior is well in line with the one predicted by our theory and shown in Figure 4a.

For the case of strong selectivity, $\chi = 4.0$, again we find a qualitatively different τ vs B behavior (see Figure 9), which agrees quite well, however, with the theoretical predictions (Figure 4b). For a given intensity of the dragging force one observes a nonmonotonic change of τ with increasing block size M with a local maximum around $M \approx 4$. Thus, one could conclude that our computer experiments provide a strong support for the theoretical model, developed in section 2 on the grounds of simple scaling considerations.

Eventually, before the end of this section we would like to point out several additional results which are believed to underline the consistency of the present combination of analytic and simulational results. An important question concerns the impact of the starting conformation of the copolymer on the observed non-Arrhenian τ vs Bl/k_BT relationship. To this end in Figure 10 we display a comparison of the measured $\tau(B)$ dependence for chains which are localized and fully equilibrated at the liquid−liquid interface before the drag force is switched on and chains with identical N and M which traverse the phase boundary "on the fly". As one may readily verify from Figure 10, for strong fields, $B \geq 0.03$, the chains which start from equilibrated position at the interface need somewhat shorter time τ to cross it than those arriving from the upper half of the simulation box. This appears reasonable since the former chains "save" the time interval between first touch of the interface whereby their center of mass still lags behind at $Z_{c.m.} \approx R_g$ above the separation line and the moment when their center of mass arrives at the interface, $Z_{c.m.} \approx 0$. For sufficiently small forces, however, one can see in Figure 10 that both curves merge; that is, the time of residence at the interface is so long that the small temporal advantage for a chain starting from the interface is completely lost. Both in the case of "equilibrated" and "on the fly" chains, however, qualitatively the τ vs Bl/k_BT relationship and its non-Arrhenian type remains unaltered, which justifies the use of equilibrium free energy expressions for the copolymer in our theoretical treatment.

Another question which pertains to the specific mechanism of copolymer detachment from the interface concerns the role of free (dangling) ends which are expected to facilitate the process of detachment. A comparison between linear chains of a given length, say $N = 128$, and ring copolymers of the same length might thus exposes the role of free chain ends. From Figure 10 one can see that for strong forces, $B \geq 0.025$, the translocation time is about 50% shorter in the case of ring, whereas for $B \leq 0.025$ it becomes gradually considerably larger than for linear chains with dangling ends. Indeed, for strong fields when the objects do not have sufficient time to localize at the interface the ring polymer crosses faster the borderline between the solvents because its size is smaller than that of the linear chain. In this regime the polymers move as almost compact objects, and the presence of free ends does not affect the mechanism of interface crossing. In contrast, for weak forces the polymers have sufficient time to localize and equilibrate on the interface while being dragged through it. The effort to tear

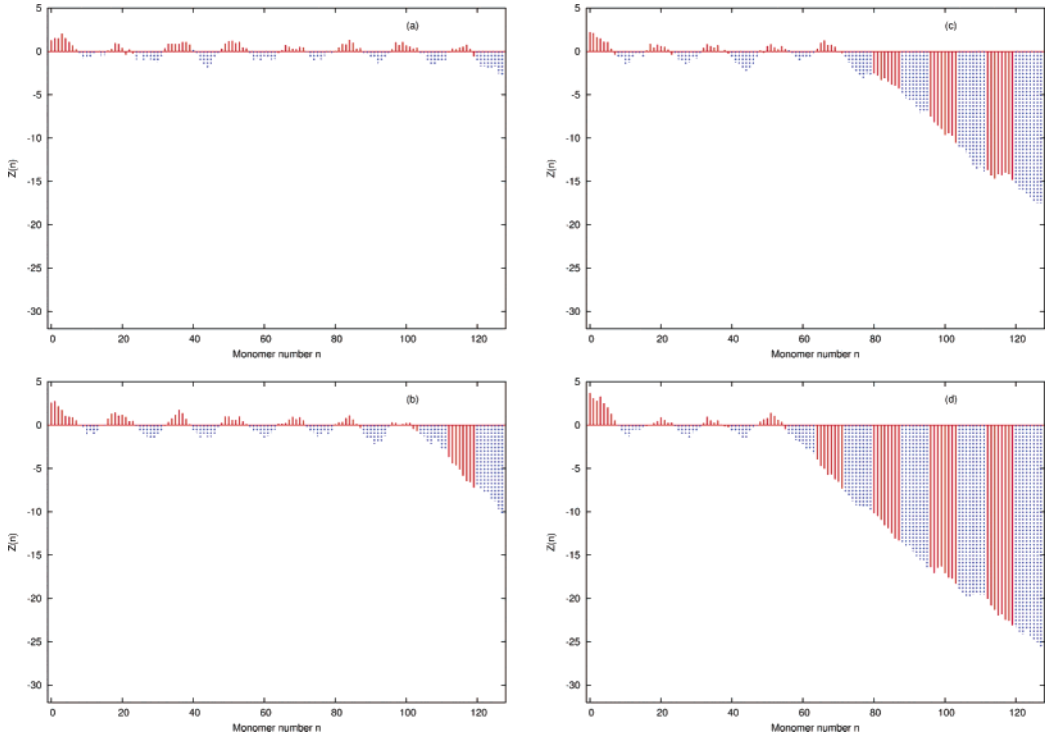

Figure 7. Snapshots showing the time evolution of the copolymer detachment from a liquid−liquid interface for a chain with $N = 128$ and $M = 8$ (different blocks are represented by solid and dashed lines) at $= 1.5$. Displayed are the Z coordinates of all 128 monomers with respect to the position of the phase boundary at $Z = 0$. The times shown are at 325 (a), 20325 (b), 100325 (c), and 200325 MCS (d) after the start of the translocation process.

a dangling end off the interface would then be only half of what is needed to create a protrusion in a ring copolymer since the protrusion is hinged by two ends to the interface. Thus, it should not be surprising that the detachment of ring copolymers take considerably longer than that of the linear ones, as demonstrated by Figure 10.

A special case which has not been in the focus of the present investigations albeit it may serve as a check for our dynamic Monte Carlo simulation is shown in the inset of Figure 10. There we present the variation of translocation time τ with chain length N for a telechelic copolymer with fixed block size $M = 4$ whereby a constant drag force $B = 0.9$ is applied only to the head monomer of the chain. Evidently, one recovers a quadratic increase of the translocation time with length N, $\tau \propto N^2$, which is qualitatively different from our data when the external field acts on all monomers of the chain. One can easily understand this observation, however, noting that for a telechelic chain the friction force grows linearly with the number of beads N, meaning that the drift velocity slows down as N^{-1}. In addition, the characteristic size of a stretched chain should be proportional to N, too. Combination of both factors should yield a quadratic growth of τ with N, and this is indeed nicely confirmed by the simulation. This last result gives us an additional confidence in the consistency of our simulation model and the observed results.

4. Conclusions

In the present work we have studied the transition of field-driven regular block copolymers through a selective liquid−liquid interface. We have developed a simple theory based on scaling considerations which appears capable of catching the main features of the phenomenon, namely, the pronounced non-Arrhenian dependence of the mean translocation time τ on field intensity B and its extreme sensitivity with respect to the copolymer architecture, that is, the block size M. It is based on the notion that the mechanism of copolymer detachment from the interface can be modeled as an activation process whereby the copolymer is pulled out of a potential well, determined by the free energy of a localized equilibrium chain, by a progressively growing protuberance. The height of the activation barrier is shown to depend dramatically on the field strength B—for large values of Bl/k_BT the barrier height disappears, and the chain is dragged without resistance through the selective phase boundary whereas for weak fields the free energy of compressed and stretched blobs determines τ. The mean translocation time itself is tackled as a mean first passage time using the Kramer's approximation, and thus predictions for qualitatively different behavior of τ in the regimes of weak and strong selectivity are derived.

In order to check the analytic theory and provide a more comprehensive understanding of the process under investigation, we have reported on extensive simulations carried out by means of a dynamic Monte Carlo model which strongly support our findings. The simulations confirm the characteristic non-Arrhenian type of the τ vs Bl/k_BT relationship while revealing distinct differences for the cases of weak and strong selectivity of the liquid−liquid interface. One remarkable feature which is reproduced by the computer experiments is the strong sensitivity of the translocation time with respect to the block size M, whereas the total chain length N turns to have little effect on τ. This sensitivity suggests the interesting possibility to use selective liquid−liquid interfaces as a new type of chromatographic tool whereby one can "sieve", that is, separate and analyze, complex mixtures of copolymers with respect to block size M. Recently, a novel method to characterize individual blocks by means of liquid chromatography at the critical condition (LCCC)[42] has been proposed. In the present work we discuss another possibility of a new type of chromatography, based on the aforementioned results.

One should note that in the rich behavior reported above we have not included results pertaining to random copolymers at

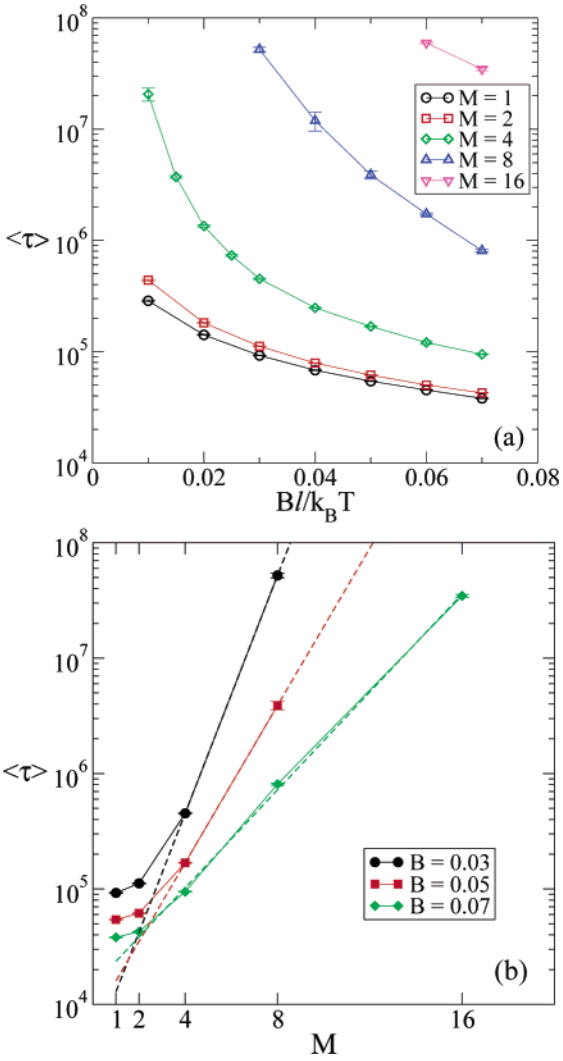

Figure 8. (a) Variation of the mean translocation time τ with field strength B for copolymers of length $N = 128$ and different block size M in the weak localization regime $\chi = 1.5$. (b) Variation of τ with block size M for $B = 0.03$, $B = 0.05$, and $B = 0.07$. An exponential fit is indicated by a dashed line.

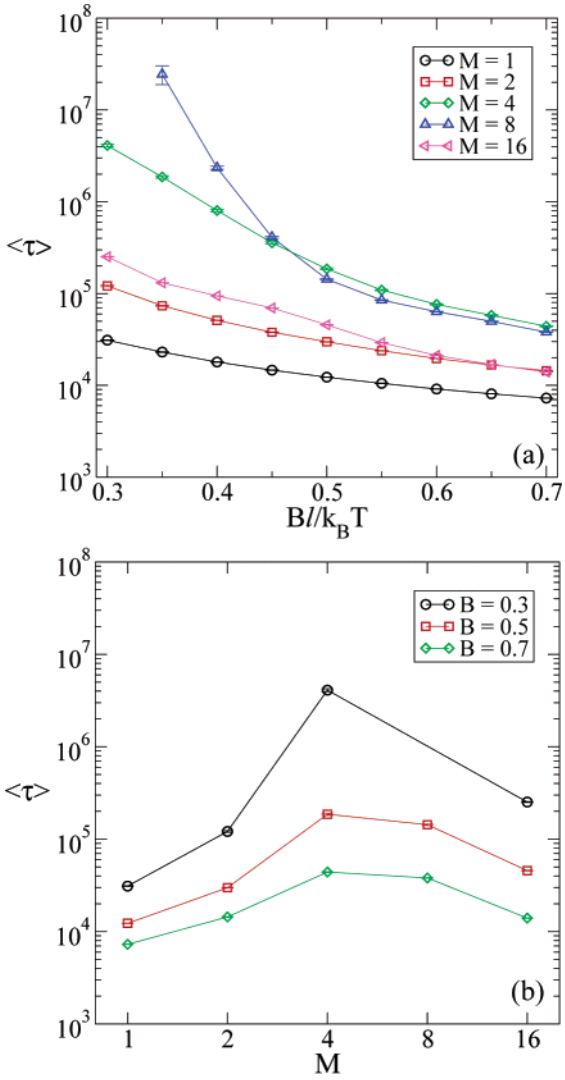

Figure 9. (a) Variation of the mean translocation time τ with field strength B for copolymers of length $N = 128$ and different block size M in the strong localization regime $\chi = 4.0$. (b) Variation of τ with block size M for $B = 0.3$, 0.5, and 0.7. As expected (cf. Figure 4b), the τ vs M relationship is, for strong selectivity, not a monotonic one.

penetrable selective interfaces where the range of sequence correlations plays a role similar to that of the block size M. Moreover, here we have totally ignored the possible effects of hydrodynamic interactions on the translocation kinetics. One might expect that the existence of a sharp interface, separating the two solvents, as well as the probable significant difference in the solvents viscosities would generally suppress hydrodynamic effects across the phase boundary. Of course, the problem becomes more complex if the presence of a copolymer at the interface changes in turn the interface properties. These are important complications which deserve a thoroughgoing investigation. Nevertheless, we could expect that the main finding about the strong sensitivity of τ with respect to M is unchanged. Eventually, this effect is evident from the localization free energy of the string of blobs (see eqs 12 and 13), where the main term grows as $F_{string} \sim -TNM^4$, i.e., strongly depends on M. Clearly, the verification of these predictions requires considerable computational efforts and therefore is on the agenda in our future work.

One should also keep in mind that all results have been derived and checked against Monte Carlo simulations within the simplest model of an interface of zero thickness. It is conceivable that by allowing for the presence of an intrinsic width of the interface as well as for a more realistic description involving capillary waves, etc., many additional facets of the general picture should become clearer. While these and other aspects imply the need of further investigations, i.e., by means of single-chain laboratory experiments, we still believe that the present study constitutes a first step into a fascinating world which might offer broad perspectives for applications and development.

Acknowledgment. A.M. acknowledges the support and hospitality of the Max-Planck Institute for Polymer Research in Mainz during this study. This research has been supported by the Sonderforschungsbereich (SFB 625).

Appendix. Calculation of the Pure Drag Time

In this Appendix we calculate the characteristic drag time for a polymer of length N pulled by an external force B along the z-axis. The calculation is based on the first passage time formula[17] which enables also to estimate $1/N$ corrections. In this case the energy field in eq 17 has the form

$$\beta U(z) = -\frac{NB}{T} z \qquad (30)$$

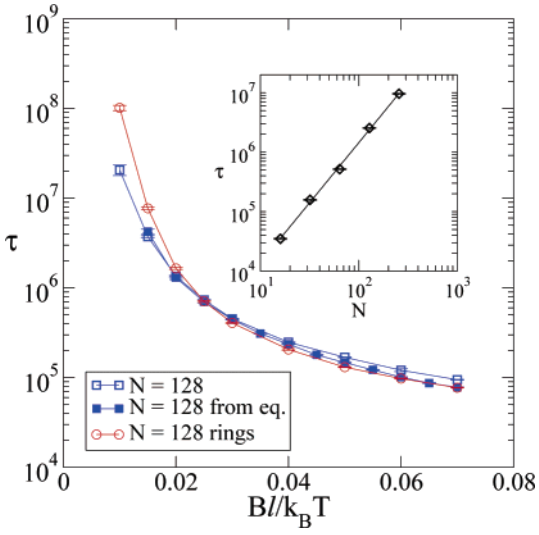

Figure 10. Variation of τ with field strength B for a chain with length $N = 128$ and block size $M = 4$. Circles denote a ring copolymer while squares mark linear chains which start from equilibrated initial conformations localized at the interface (full symbols) or enter the interface "on the fly" (empty symbols). The inset shows the variation of τ with N for a telechelic chain where the field $B = 0.9$ is applied only at the head monomer of the chain. The straight line denotes a power law, $\tau \propto N^{\beta}$, with an exponent $\beta = 2.02 \pm 0.04$.

The polymer chain center of mass starts from $z = 0$ at $t = 0$; we want to estimate the value of the time at which the center of mass of the chain passes $z = L$. According to eq 17 the average time of the first passage reads

$$\tau_{\text{drag}} = \frac{\zeta_0 N}{T}\int_0^L \mathrm{d}z' \exp\left[-\frac{NB}{T}z'\right]\int_0^{z'} \mathrm{d}z \exp\left[\frac{NB}{T}z\right] \quad (31)$$

where we have used for the diffusion coefficient its Rouse expression $D = T/\zeta_0 N$. The straightforward calculation of the integrals in eq 31 yields

$$\tau_{\text{drag}} = \frac{L\zeta_0}{B}\left\{1 - \frac{T}{NLB}\left[1 - \exp\left(-\frac{NLB}{T}\right)\right]\right\} \quad (32)$$

One can see that for a large chain, i.e. at $N \gg 1$, and for a characteristic length of the order of the blob length, i.e. at $L \simeq ag^{\nu}$, we go back to the simple expression $\tau_{\text{drag}} \simeq ag^{\nu}\zeta_0/B$. The finite chain size correction can be expressed in terms of factors proportional to powers of $[1 - T/(BLN)]$.

References and Notes

(1) Corsi, A.; Milchev, A.; Rostiashvili, V. G.; Vilgis, T. A. *J. Chem. Phys.* **2005**, *122*, 094907.
(2) Corsi, A.; Milchev, A.; Rostiashvili, V. G.; Vilgis, T. A. *Europhys. Lett.* **2006**, *73*, 204.
(3) Corsi, A.; Milchev, A.; Rostiashvili, V. G.; Vilgis, T. A. *Macromolecules* **2006**, *39*, 1234.
(4) Corsi, A.; Milchev, A.; Rostiashvili, V. G.; Vilgis, T. A. *J. Polym. Sci., Part B*, in press.
(5) Clifton, B. J.; Cosgrove, T.; Richardson, R. M.; Zarbakhsh, A.; Webster, J. R. P. *Physica B* **1998**, *248*, 289.
(6) Rother, G.; Findenegg, G. F. *Colloid Polym. Sci.* **1998**, *276*, 496.
(7) Wang, R.; Schlenoff, J. B. *Macromolecules* **1998**, *31*, 494.
(8) Omarjee, P.; Hoerner, P.; Riess, G.; Cabuil, V.; Mondain-Monval, O. *Eur. Phys. J. E* **2001**, *4*, 45.
(9) Sommer, J.-U.; Daoud, M. *Europhys. Lett.* **1995**, *32*, 407.
(10) Sommer, J.-U.; Peng, G.; Blumen, A. *J. Phys. II* **1996**, *6*, 1061.
(11) Garel, T.; Huse, D. A.; Leibler, S.; Orland, H. *Europhys. Lett.* **1998**, *8*, 9.
(12) Chatellier, X.; Joanny, J.-F. *Eur. Phys. J. E* **2000**, *1*, 9.
(13) Denesyuk, N. A.; Erukhimovich, I. Ya. *J. Chem. Phys.* **2000**, *113*, 3894.
(14) Balasz, A. C.; Semasko, C. P. *J. Chem. Phys.* **1990**, *94*, 1653.
(15) Israels, R.; Jasnow, D.; Balazs, A. C.; Guo, L.; Krausch, G.; Sokolov, J.; Rafailovich, M. J. *Chem. Phys.* **1995**, *102*, 8149.
(16) Sommer, J.-U.; Peng, G.; Blumen, A. *J. Chem. Phys.* **1996**, *105*, 8376.
(17) Lyatskaya, Y.; Gersappe, D.; Gross, N. A.; Balazs, A. C. *J. Chem. Phys.* **1996**, *100*, 1449.
(18) Chen, Z. Y. *J. Chem. Phys.* **1999**, *111*, 5603; **2000**, *112*, 8665.
(19) Pincus, P. *Macromolecules* **1976**, *9*, 386.
(20) Brochard-Wyart, F. *Europhys. Lett.* **1993**, *23*, 105.
(21) Brochard-Wyart, F.; Hervet, H.; Pincus, P. *Europhys. Lett.* **1994**, *26*, 511.
(22) Brochard-Wyart, F. *Europhys. Lett.* **1995**, *30*, 387.
(23) Avramova, K.; Yamakov, V.; Milchev, A. *Macromol. Theory Simul.* **2000**, *9*, 516.
(24) Risken, H. *The Fokker-Planck Equation*; Springer-Verlag: Berlin, 1989.
(25) Weiss, G. H. *Adv. Chem. Phys.* **1966**, *13*, 1.
(26) van Kampen, N. G. *Stochastic Processes in Physics and Chemistry*; North-Holland: Amsterdam, 1992.
(27) Sung, W.; Park, P. J. *Phys. Rev. Lett.* **1996**, *77*, 783.
(28) Park, P. J.; Sung, W. *J. Chem. Phys.* **1998**, *108*, 3013.
(29) Park, P. J.; Sung, W. *Phys. Rev. E* **1998**, *57*, 730.
(30) Muthukumar, M. *J. Chem. Phys.* **1999**, *111*, 10371.
(31) Milchev, A.; Binder, K.; Bhattacharya, A. *J. Chem. Phys.* **2004**, *121*, 6042.
(32) Milchev, A.; Paul, W.; Binder, K. *J. Chem. Phys.* **1993**, *99*, 4786.
(33) Milchev, A.; Binder, K. *Macromol. Theory Simul.* **1994**, *3*, 915.
(34) Milchev, A.; Binder, K. *J. Chem. Phys.* **2001**, *114*, 8610.
(35) Milchev, A.; Milchev, A. *Europhys. Lett.* **2001**, *56*, 695.
(36) Milchev, A.; Binder, K. *Macromolecules* **1996**, *29*, 343.
(37) Milchev, A.; Binder, K. *J. Phys. II* **1996**, *6*, 21; *Eur. Phys. J. B* **1998**, *9*, 477.
(38) Pandey, R. B.; Milchev, A.; Binder, K. *Macromolecules* **1997**, *30*, 1194.
(39) Milchev, A.; Binder, K. *J. Chem. Phys.* **1997**, *106*, 1978.
(40) Gerroff, I.; Milchev, A.; Paul, W.; Binder, K. *J. Chem. Phys.* **1993**, *98*, 6526.
(41) Milchev, A.; Wittmer, J.; Landau, D. P. *Eur. Phys. J. B* **1999**, *12*, 241.
(42) Jiang, W.; Khan, S.; Wang, Y. *Macromolecules* **2005**, *38*, 7514.

MA060920N